



## ARTICLE

# Improving Heat Transfer in Parabolic Trough Solar Collectors by Magnetic Nanofluids

Ritesh Singh<sup>1</sup>, Abhishek Gupta<sup>1</sup>, Akshoy Ranjan Paul<sup>1,\*</sup>, Bireswar Paul<sup>1</sup> and Suvash C. Saha<sup>2,\*</sup>

<sup>1</sup>Department of Applied Mechanics, Motilal Nehru National Institute of Technology Allahabad, Prayagraj, India

<sup>2</sup>Department of Mechanical and Mechatronic Engineering, University of Technology Sydney, Sydney, Australia

\*Corresponding Authors: Akshoy Ranjan Paul. Email: arpaul@mnnit.ac.in; Suvash C. Saha. Email: Suvash.Saha@uts.edu.au

Received: 17 October 2023 Accepted: 18 January 2024 Published: 26 March 2024

## ABSTRACT

A parabolic trough solar collector (PTSC) converts solar radiation into thermal energy. However, low thermal efficiency of PTSC poses a hindrance to the deployment of solar thermal power plants. Thermal performance of PTSC is enhanced in this study by incorporating magnetic nanoparticles into the working fluid. The circular receiver pipe, with dimensions of 66 mm diameter, 2 mm thickness, and 24 m length, is exposed to uniform temperature and velocity conditions. The working fluid, Therminol-66, is supplemented with Fe<sub>3</sub>O<sub>4</sub> magnetic nanoparticles at concentrations ranging from 1% to 4%. The findings demonstrate that the inclusion of nanoparticles increases the convective heat transfer coefficient (HTC) of the PTSC, with higher nanoparticle volume fractions leading to greater heat transfer but increased pressure drop. The thermal enhancement factor (TEF) of the PTSC is positively affected by the volume fraction of nanoparticles, both with and without a magnetic field. Notably, the scenario with a 4% nanoparticle volume fraction and a magnetic field strength of 250 G exhibits the highest TEF, indicating superior thermal performance. These findings offer potential avenues for improving the efficiency of PTSCs in solar thermal plants by introducing magnetic nanoparticles into the working fluid.

## KEYWORDS

Parabolic trough solar collector (PTSC); magnetic nanofluid (MNF); heat transfer; convective heat transfer coefficient (HTC); thermal enhancement factor (TEF)

## Nomenclature

$\vec{B}$	Magnetic flux density
$C_p$	Coefficient of specific heat, J/Kg K
$D_i$	Inner diameter of collector tube, m
$f$	Friction factor
$h$	Heat transfer rate, W/m <sup>2</sup> K
$\vec{H}$	Magnetic field intensity
$k$	Thermal conductivity, W/m K
$L$	Length of the absorber tube, m
$\vec{M}$	Magnetization
Nu	Nusselt number



This work is licensed under a Creative Commons Attribution 4.0 International License, which permits unrestricted use, distribution, and reproduction in any medium, provided the original work is properly cited.

Re	Reynolds number
$u, U$	Flow velocity, m/s
$\vec{v}$	Velocity of ferrofluid, m/s
$\Delta P$	Pressure drop, Pa
$\mu$	Coefficient of dynamic viscosity, kg/m s
$\mu_0$	Magnetic permeability of the medium
$\nu$	Dynamic viscosity, m <sup>2</sup> /s
$\rho$	Density, kg/m <sup>3</sup>

## 1 Introduction

The pursuit of renewable energy has become paramount in countering the escalating demand for electricity and the concerning surge in greenhouse gas emissions across the globe. Countries like India, China, and the US have veered toward investing heavily in solar, wind, hydro, and biofuel technologies to address this pressing issue. By 2030, an estimated 800,000 MW of additional electricity generation capacity will be imperative, with renewable sources anticipated to play a pivotal role in meeting this demand. Solar energy stands out as a frontrunner capable of supplanting traditional energy sources, presenting an opportunity to curtail energy consumption while fortifying ecosystems against pollution and the perils of global warming.

India's National Solar Mission stands as a testament to this paradigm shift, aiming not only to diminish the nation's reliance on fossil fuels but also to propel its economic modernization. As part of this initiative, research endeavors are underway to bolster India's ambition of significantly augmenting its installed capacity with intensive solar power plants by the targeted year of 2030 [1].

Among the various technologies, solar thermal power plants leverage solar collectors to harness solar radiation and convert it into usable energy. Parabolic trough collectors (PTCs), such as those employing magnetic nanofluids (MNFs), exhibit remarkable efficacy in harvesting solar energy. The MNFs are formed by dispersing magnetic nanoparticles in a base fluid, combining the properties of nanoparticles and base fluid. The presence of an externally applied magnetic field can modify the flow and heat transmission properties of MNFs. Common metals used for magnetic nanoparticles include iron, nickel, cobalt, and magnetite. The enhancement of thermal conductivity in solar collectors becomes achievable through the integration of MNFs and the application of an external magnetic field, consequently leading to escalated heat transfer rates. Moreover, the magnetic field's influence extends to regulating the viscosity of the nanofluid. An array of research initiatives has focused on optimizing parabolic solar trough collectors (PTSCs), encompassing factors like internal fins, geometrical alterations, materials, porous structures, nanofluids, and methods to induce turbulence [2–6].

Ample evidence from various studies underscores the potential of nanofluids to significantly bolster heat transfer efficiency in thermal systems [7]. For instance, aluminum oxide-based nanofluids exhibited a 3.90% efficiency surge in a parabolic trough collector, with configurations featuring two circular categories surpassing uniform nanofluids, resulting in a notable 12.5% efficiency elevation [7,8].

Further investigations into alumina-water nanofluid unveiled a staggering 47% increase in heat transfer rates, while CNT/water nanofluid demonstrated a remarkable 3.5 times enhancement, and CuO/water nanofluid showcased a commendable 25% heat transfer augmentation [9–11]. Intriguingly, the characteristics of the base fluid themselves exerted an impact on thermal conductivity enhancement, with the lowest initial thermal conductivity exhibiting the most pronounced improvement [12].

Magnetic Nanofluids (MNFs) represent a fusion of magnetic nanoparticles within a base fluid, amalgamating the properties of both components. The introduction of an externally applied magnetic field can dynamically alter the flow and heat transmission attributes of MNFs. Magnetic nanoparticles, including iron, nickel, cobalt, and magnetite, have commonly been used in this context. Studies have shown that magnetic fields enhance heat transfer in MNFs. Jafari et al. [13] found that magnetic fields increased the HTC and Nusselt number in kerosene-based nanofluids, while nanoparticle agglomeration reduced it. Li et al. [14] and Lajavardi et al. [15] found that magnetic fields improved heat transfer rates in heated wire and laminar flows with  $\text{Fe}_3\text{O}_4$ -based ferrofluids. Sheikholeslami et al. [16] found that raising the Hartmann number reduced the nanofluid's velocity and heat transfer rate, with platelet-shaped nanoparticles providing the highest heat transfer rate. The effect of magnetic fields on convective HTC was studied using numerical simulations. Ebraze et al. [17] found that nanofluids can improve solar panel efficiency, particularly in photo-thermal solar collectors. Cao et al. [18] found that increased absorber surface area increased convective heat transfer (CHT), leading to higher outlet temperatures. Khosravi et al. [19] found that collector's HTC increased with higher nanoparticle suspensions and magnetic field intensity. Malekan et al. [2] found that  $\text{CuO}$ /Therminol-66 and  $\text{Fe}_3\text{O}_4$ /Terminal-66-based nanofluids increased collector efficiency by up to 4% at 1% particle concentration in PTSC under an external magnetic field.

The integration of MNFs into solar thermal systems emerges as a promising avenue to bolster efficiency and elevate the efficacy of solar power plants. The synergy between magnetic fields and nanofluids presents a compelling prospect in revolutionizing solar energy harvesting, advancing us toward a more sustainable energy landscape. The literature review assesses factors affecting the energetic and exergetic performance of MNF-based solar collectors, identifying research gaps like limited experimental studies, limited understanding of nanofluid configurations, and limited comparisons between different types. The use of conventional barriers like turbulators, baffles, vortex generators create turbulence in the working fluid but at the cost of high parasitic pressure losses. Our goal is to address this issue by employing an external magnetic field. Utilizing MNFs offers a significant advantage as they respond to this external magnetic field. Consequently, this magnetic field becomes instrumental in inducing turbulence within the fluid flow, thereby amplifying heat transfer while minimizing parasitic pressure losses. The present study, therefore, investigated the use of MNFs in PTSCs, focusing on heat transfer modes and radiation losses. It numerically analyzes PTSC performance under a constant external magnetic field and computes the impact of magnetic field, local HTC, Reynolds number, nanoparticles, and nanofluid volume fraction on flow.

## 2 Materials and Methods

This section describes the computational methodology and the validation of the CFD solver in the following sub-sections.

### 2.1 Geometric Modeling and Grid Generation

A PTSC uses U-shaped mirrors to harvest solar radiation, converting it into thermal energy. MNFs are evaluated using CFD modelling to improve collector thermal performance. The PTSC system model, shown in Fig. 1, involves a parabolic concentrator which concentrates solar radiation into a receiver tube and transmitting it to a MNF for heat transfer. The semi-cylindrical tube has a symmetrical layout, consisting of an outer layer as a solid wall and an inner section as a fluid conduit. The circular receiver tube of the PTSC considered has an inner diameter of 66 mm with 2 mm thickness and 24 m in length.

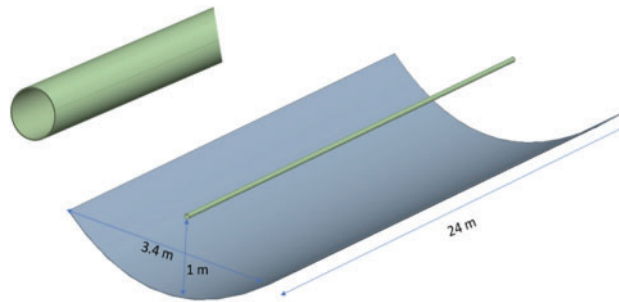


**Figure 1:** Computational domain of the proposed model of parabolic trough solar collector

Fig. 2 depicts the structured mesh in the collecting tube. Grid generation was carried out in Ansys software. Grid sensitivity is an important part of the numerical investigation. In order to test the grid sensitivity, the values of heat transfer coefficient is monitored. The Grid independence test is performed with  $Re = 15000$ , a uniform heat flux, and working fluid (magnetic nanofluid-1%) and is furnished in Fig. 3. Finally, grid with elements 1219301 is found to be suitable for this study.

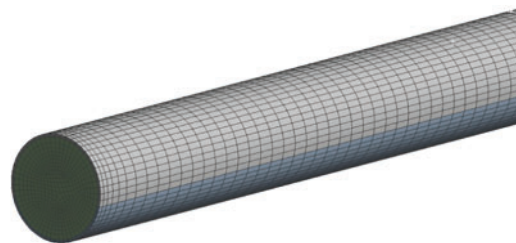


**Figure 2:** Structured meshing of the collector tube

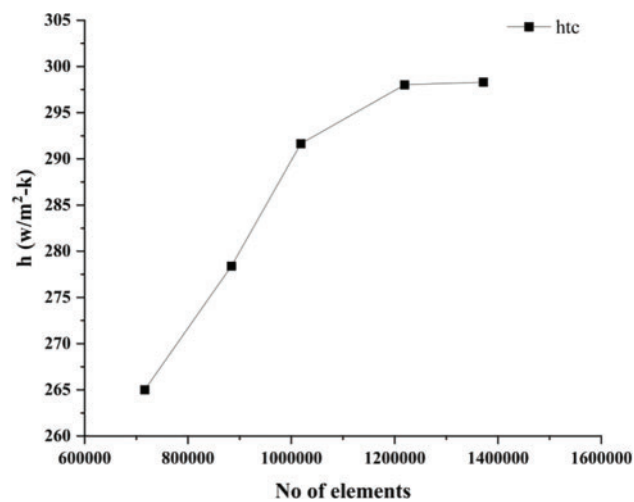


**Figure 3:** Grid independence test

### 2.2 Working Fluid Parameters

The nanoparticles volume fraction (volume percentage, i.e., 1%–4%) affects the characteristics of MNFs. The magnetic nanofluid characteristics may be calculated using a sequence of equations based on the physical properties of nanoparticles and base fluid, as shown in Table 1 [20–22].

**Table 1:** Thermophysical properties of base fluid and magnetic nanofluid

Material	$\rho$ (kg/m <sup>3</sup> )	$C_p$ (J/kg K)	$k$ (W/m K)	$\mu$ (kg/m s)
Base fluid (Themamol-66)	899.5	2122	0.107	0.00106
Fe <sub>3</sub> O <sub>4</sub> nanoparticle	5200	670	6	
Magnetic nanofluid (1%)	942.5	2107.48	0.110073	0.0010865
Magnetic nanofluid (2%)	985.5	2092.96	0.113206	0.001113
Magnetic nanofluid (4%)	1071.5	2063.92	0.119657	0.001166

### 2.3 Governing Equations

The MNF is considered as a single-phase fluid and its physical and chemical properties are determined by the concentration of base fluid and nanoparticles. The continuity, energy, and momentum equations of a base fluid apply to MNF, except that the effective properties must exchange for the base fluid’s properties. Conservation equations can be described as follows:

*Continuity equation:*

$$\nabla \cdot (\rho_{nf} \vec{v}) = 0 \tag{1}$$

where  $\rho_{nf}$  defines the nanofluid density, kg/m<sup>3</sup>,  $\vec{v}$  defines the velocity of ferrofluid, m/s.

*Momentum Equation:*

$$\nabla \cdot (\rho_{nf} \vec{v}) = -\nabla p + \nabla \cdot (\mu_{nf} \nabla \vec{v}_{nf}) + \mu_0 (\vec{M} \cdot \nabla) \vec{H} \tag{2}$$

where  $\mu_0$  denotes the magnetic permeability. The term  $\mu_0 (\vec{M} \cdot \nabla) \vec{H}$  denotes the Kelvin force, N.

Maxwell equation was used to calculate the magnetic flux density ( $\vec{B}$ ) as follows:

$$\vec{B} = \mu_0 (\vec{M} + \vec{H}) \tag{3}$$

where  $\vec{M}$  is the magnetization,  $\vec{H}$  is the magnetic field intensity and  $\mu_0$  is the permeability of the medium.

*Energy Equation:*

$$\rho_{nf} C_{p,nf} \left( \frac{\partial T}{\partial t} + \vec{v}_{nf} \cdot \nabla T \right) = k_{nf} \nabla^2 T, \tag{4}$$

The parameters used to calculate thermal efficiency of the system are:

*Nusselt Number (Nu):*

The ratio of the convective heat transfer to the conductive heat transfer in a system is expressed as the Nusselt number, a dimensionless metric. It is the ratio of the heat flow rate via conduction through

a constant thickness at the same temperature differential to the convective heat transfer rate.

$$Nu = \frac{hD_i}{k}, \quad (5)$$

where  $h$  defines the heat transfer rate, W/m<sup>2</sup> K,  $D_i$  defines inner diameter of collector tube, m,  $k$  denotes the thermal conductivity, W/m K.

*Reynolds Number (Re):*

A fluid's flow regime in a pipe or channel can be described by a dimensionless quantity called the Reynolds number. It uses the fluid's inertia force in relation to its viscous force to determine laminar or turbulent flow.

$$Re = \frac{UD_i}{\nu}, \quad (6)$$

where  $U$  denotes the flow velocity, m/s,  $\nu = \frac{\mu}{\rho}$ , where the  $\nu$  is dynamic viscosity, m<sup>2</sup>/s.

*Friction Factor (f):*

The friction factor, a measure of fluid flow resistance, can be used to calculate the pressure loss along the receiver pipe. It reveals how the fluid loses energy and experiences a pressure drop as it travels through the pipe.

$$f = \frac{2\Delta P}{\rho_{nf}u^2} \left( \frac{D_i}{L} \right), \quad (7)$$

where  $\Delta P$  denotes the pressure drop, Pa,  $\rho_{nf}$  denotes the density of nanofluids, kg/m<sup>3</sup>,  $u$  defines the velocity of fluid, m/s,  $L$  denotes the length of the absorber tube, m.

Theoretically, friction factor can also be calculated from Petukhov relation:

$$f = \frac{1}{(0.79 \ln Re - 1.64)} \quad (8)$$

*Thermal Enhancement Factor (TEF):*

The efficiency of heat transfer can be measured with a statistic called the thermal enhancement factor. It indicates the improvement in heat transfer rate per unit change in friction factor. The thermal enhancement factor is a crucial factor in optimizing heat transfer systems, indicating a more efficient process with a higher heat transfer rate. It helps identify effective techniques and configurations to enhance heat transfer while minimizing frictional losses.

$$TEF = \frac{Nu_{nf}}{\left( \frac{f_{nf}}{f_b} \right)^{1/3}}, \quad (9)$$

where  $Nu_{nf}$  denotes the nanofluids Nusselt number,  $Nu_b$  define the base fluid Nusselt number,  $f_{nf}$  denotes the nanofluid friction factor and  $f_b$  is the base fluid friction factor.

## 2.4 Boundary Conditions

Table 2 represents initial and boundary conditions and solver setting used in the study.

**Table 2:** Boundary conditions and CFD solver settings for the model

Numerical model	Conditions	Value
Energy equation	on	
Turbulence model	RNG $k-\epsilon$	
MHD model	on	
Boundary conditions		
Inlet	Velocity inlet	$Re = 1 \times 10^4$ to $2.6 \times 10^5$
Outlet	Gauge pressure	0 Pa
Upper wall	Wall	
	Heat flux	700 W/m <sup>2</sup>
Down wall	Wall	
	Heat flux	19500 W/m <sup>2</sup>

**2.5 Validation**

The Fig. 4 shows the heat transfer coefficient variation produced from the present simulation. The current simulation results of 1% nanofluids are compared to numerical results obtained from Sami et al. [23]. The numerical outcome agreed well with the correlation with a maximum deviation 6.87% indicating that the present numerical model is reliable.

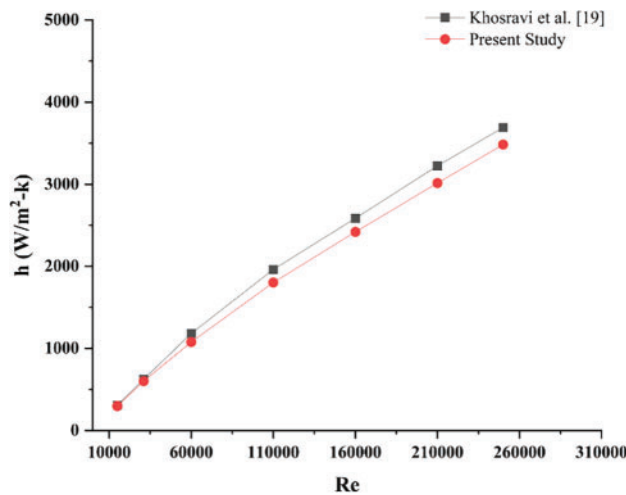


**Figure 4:** Comparison of heat transfer coefficient with Reynolds number

Fig. 5 shows the friction factor variation produced from the present simulation. As can be observed in this graph, the current CFD results are in good agreement even with the theoretical outputs (i.e., Petukhov correlation mentioned in Eq. (8)), with a maximum deviation of 2.23% indicating that the present numerical model is reliable.

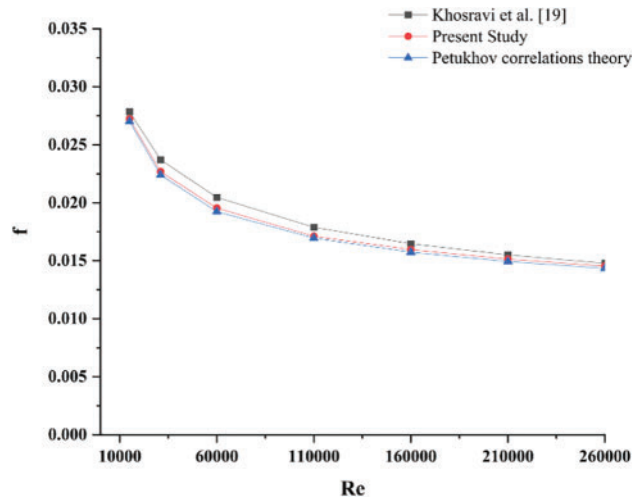


**Figure 5:** Comparison of friction factor with Reynolds number

### 3 Results and Discussion

This study examines the effects of circumferential heating, magnetic field, and fluid types such as Therminol-66 and MNF on HTC, Nusselt number, friction factor, pressure decreases, and TEF. Fig. 6 depict the local HTC for various nanofluid volume fractions (1% to 4%) with or without a magnetic flux density (B). In MNF, the local HTC increases as the volume fraction of  $\text{Fe}_3\text{O}_4$  nanoparticles increases.

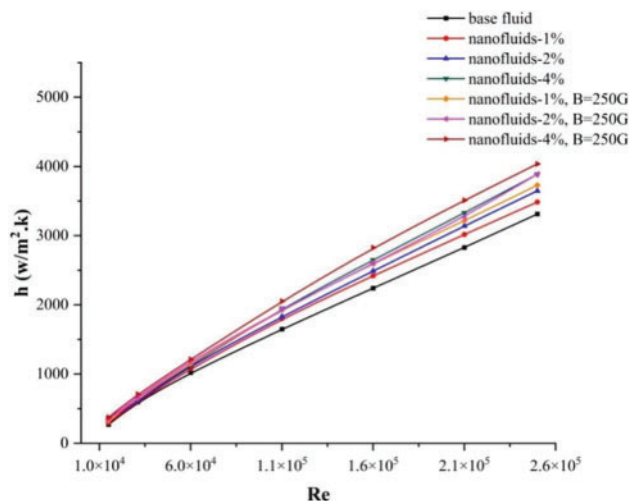


**Figure 6:** Heat transfer coefficient of nanofluid with magnetic field for all cases,  $h$  vs.  $Re$

The local HTC increased with a rise in Reynolds number for both the MNF and the base fluid in an applied transverse magnetic field, as shown in Fig. 6. In the absence of a magnetic field, HTC of MNF is greater than that of base fluid, indicating that dispersed particles in the base fluid contribute to an improvement in HTC of the collecting tube.

Fig. 7 illustrates how a magnetic field and nanoparticles affect the fluctuation of the Nu. As the Reynolds number increased, both the MNF and the base fluid exhibited an increase in the Nu. In addition, the MNF exhibited a greater Nu than the basal fluid. This can be explained by the fact that the nanoparticles in the MNF have a higher thermal conductivity. Nu exhibited an upward trend with increasing nanoparticle volume fractions, ranging from 1% to 4%, indicating that as the nanoparticle volume fraction in-creased, the thermal conductivity of the nanofluid improved, resulting in a higher Nu.

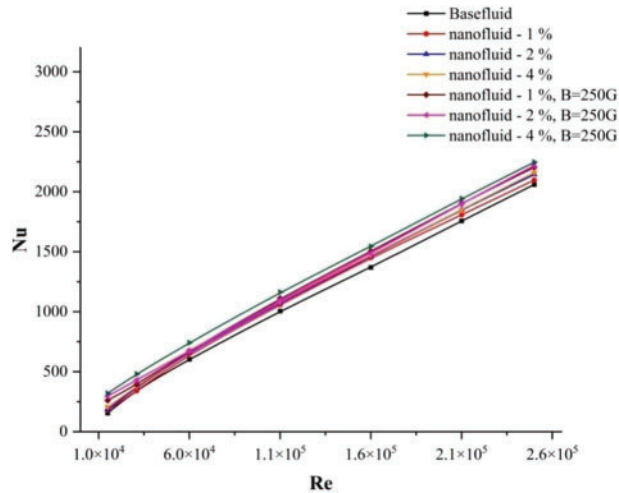


Figure 7: Impact of magnetic field on the Nusselt number, Nu vs. Re

Fig. 8 depicts the interaction between friction factor and Re. The friction factor is discovered to be impacted by varied volume fraction percentages of MNF in the receiver pipe, both with and without magnetic field. The friction factor decreases as Re increases for all nanofluid cases. The friction factor of MNF is larger than that of the base fluid as a result of its increased viscosity as well as its increased density.

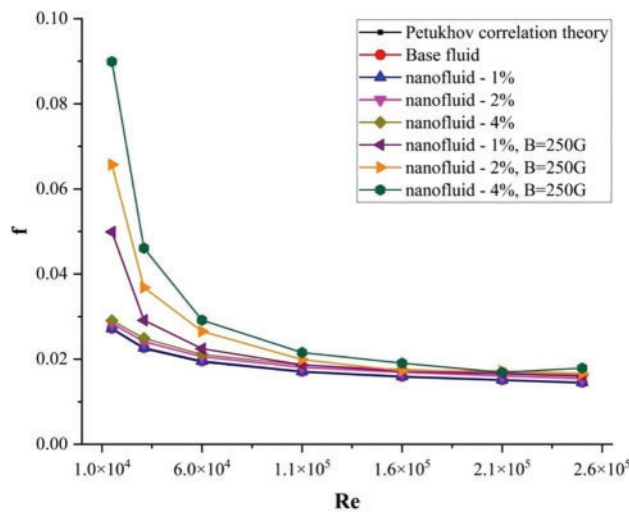
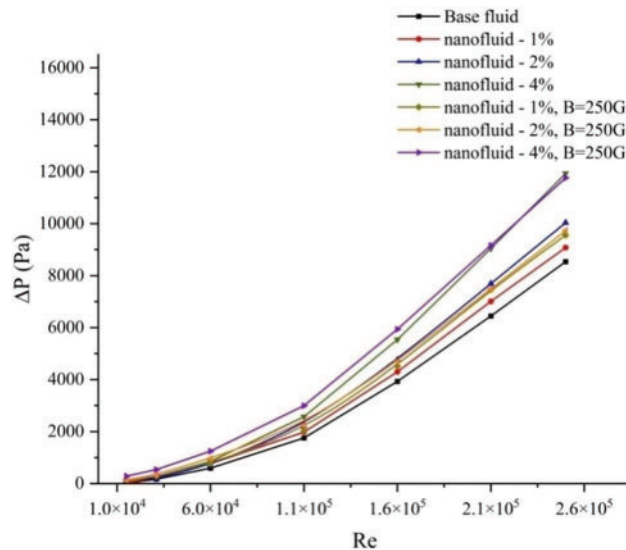


Figure 8: Impact of magnetic field on the friction factor, *f* vs. Re

Similarly, the pressure drop experienced by the MNF is influenced by the differing volume fraction percentages of the nanofluid and base fluid in the receiver pipe. Fig. 9 illustratively demonstrates this. The viscosity of the MNF increases as nanoparticles are infused to the base fluid. This results a significant pressure drop, especially for higher volume fractions. In addition, as the Re increases, the pressure loss rises as a result of the increased nanofluid velocities caused by larger Reynolds numbers. As depicted in Fig. 6, an increase in pressure drop corresponds to a rise in  $f$ .



**Figure 9:** Variation of pressure drop for nanofluid and base fluid,  $\Delta P$  vs. Re

It is crucial to compute the overall improvement in thermal performance in order to establish whether or not the combination of a magnetic field and a nanofluid could have any practical applications. The TEF is used to evaluate this improvement, outlined by Eq. (9). Fig. 10 depicts the fluctuation of TEF with Re for various volume fractions of MNF and base fluid in the receiver conduit, both with and without the magnetic field. The results indicate that TEF of the collector rises as the volume fraction of MNF increases. This enhancement is due to the MNF's improved thermal conductivity. Additionally, the presence of a magnetic field is demonstrated to improve heat transfer performance as seen by an increase in the TEF.

The collector achieves highest possible value for its TEF when a MNF with a volume percentage of 4% is used while also being in the presence of a magnetic field. Based on these findings, it appears that an improvement of a significant amount in thermal performance can be achieved by combining a magnetic field with a greater volume percentage of MNFs.

The temperature distribution at the collector tube's outlet is shown in Fig. 11. The figure shows the outlet temperature of both the base fluid and MNFs with a 4% volume fraction when the inlet temperature is 503 K and the Reynolds number is 15000. The surface temperature of the collection tube is higher when no magnetic field was present. Convective transfer of heat is significantly enhanced by secondary flows and the creation of vortices within the collection tube, as observed here. The enhanced convective heat transfer is a direct result of intense flow mixing.

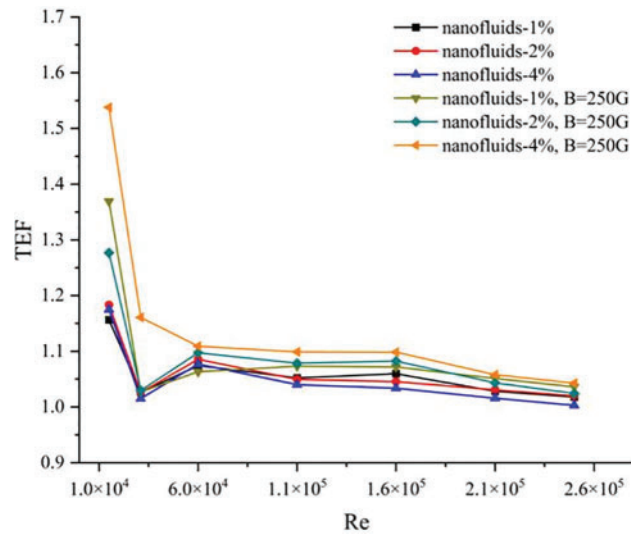


Figure 10: Thermal enhancement factor with different magnetic nanofluids and base fluid

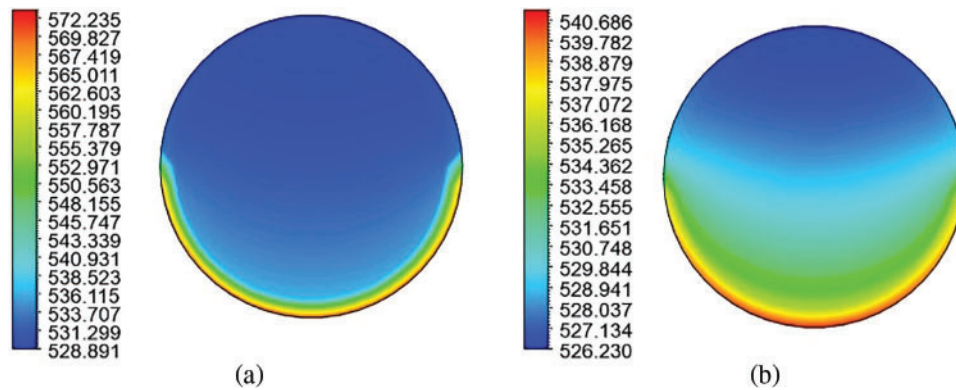


Figure 11: Outlet temperature contour at  $Re = 15000$ , (a) base fluid (therminol-66) (b) magnetic nanofluid-4%

#### 4 Conclusions

The research investigated how the combination of magnetic nanofluid (MNF) and a magnetic field affected the thermal efficiency of a PTSC. Using computational fluid dynamics, the study examined various factors' impact on convective heat transfer coefficients (HTC) and thermal efficiency. From this analysis, several key conclusions emerged. Introducing an external magnetic field and MNFs resulted in higher heat transfer coefficients and Nusselt numbers compared to scenarios without magnetic fields. Incorporating nanoparticles into the base fluid boosted the HTC of the solar collector, which increased further with higher nanoparticle volume fractions. Among the cases studied, the MNF with a 4% nanoparticle volume fraction and a magnetic flux density of  $B = 250$  G displayed the most significant thermal performance. Regardless of the magnetic field's presence, friction factors decreased as Reynolds numbers rose. Moreover, the thermal efficiency factor of the collector rose with escalating nanoparticle volume fractions in the MNF. These findings highlight the potential for leveraging MNFs and magnetic fields to enhance PTSCs' thermal performance, bolstering their practical application in solar energy systems.

While a wealth of numerical simulation-based research papers delves into external magnetic field-based parabolic trough solar collectors (PTSCs), there remains a significant scarcity in experimental work within this domain. Notably, only a handful of researchers [23,24] have documented laboratory-scale experimental models of solar collectors influenced by external magnetic fields. Surprisingly, the open literature lacks substantial information pertaining to the practical application of these models within commercial, industrial, or large-scale settings. The dearth of available data concerning the implementation and scalability of these technologies in real-world scenarios represents a significant gap in the current knowledge landscape. Implementing MNFs in solar energy systems requires thorough investigation, focusing on scaling up the technology and evaluating its viability in real-world scenarios. Long-term stability, cost-effectiveness, and environmental impact are essential aspects that future research should address to facilitate the practical integration of MNFs in solar energy systems. Further, the future study may also include developing precise models to accurately represent the true behavior of MNFs, refining existing models to encompass rheological and thermophysical traits, examining how nanoparticle size and shape affect thermal conductivity and heat transfer, and modeling interactions between nanoparticles to optimize thermal performance.

**Acknowledgement:** The authors acknowledge MNNIT Allahabad and UTS Sydney for facilitating the work.

**Funding Statement:** The authors received no specific funding for this study.

**Author Contributions:** The authors confirm contribution to the paper as follows: study conception and design: AR Paul, B Paul; analysis and interpretation of results: AR Paul, R Singh; numerical simulations: R Singh, A Gupta; draft manuscript preparation: R Singh, A Gupta; manuscript edit: SC Saha, AR Paul, B Paul. All authors reviewed the results and approved the final version of the manuscript.

**Availability of Data and Materials:** The data related to the manuscript are available with the communicating authors and can be made available to the interested readers upon reasonable request.

**Conflicts of Interest:** The authors declare that they have no conflicts of interest to report regarding the present study.

## References

1. Gupta, A., Paul, A. R., Saha, S. C. (2023). Decarbonizing atmosphere using carbon capture, utilization, and sequestration: Challenges, opportunities, and policy implications in India. *Atmosphere*, 14(10), 1546. <https://doi.org/10.3390/atmos14101546>
2. Malekan, M., Khosravi, A., Syri, S. (2019). Heat transfer modeling of a parabolic trough solar collector with working fluid of Fe<sub>3</sub>O<sub>4</sub> and CuO/Therminol 66 nanofluids under magnetic field. *Applied Thermal Engineering*, 163, 114435. <https://doi.org/10.1016/j.applthermaleng.2019.114435>
3. Khetib, Y., Alahmadi, A., Alzaed, A., Sharifpur, M., Cheraghian, G. et al. (2021). Simulation of a parabolic trough solar collector containing hybrid nanofluid and equipped with compound turbulator to evaluate exergy efficacy and thermal-hydraulic performance. *Energy Science & Engineering*, 9, 897–915. <https://doi.org/10.1002/ese3.867>
4. Abu-Hamden, N. H., Abusorrah, A. M., Bayoumi, M. M., Oztop, H. F., Sun, C. (2021). Numerical study on heat loss from the surface of solar collector tube filled by oil-NE-PCM/Al<sub>2</sub>O<sub>3</sub> in the presence of the magnetic field. *Journal of Thermal Analysis and Calorimetry*, 144(6), 2627–2639. <https://doi.org/10.1007/s10973-020-09689-3>

5. Norouzi, A. M., Siavashi, M., Oskouei, M. K. (2020). Efficiency enhancement of the parabolic trough solar collector using the rotating absorber tube and nanoparticles. *Renewable Energy*, 145, 569–584. <https://doi.org/10.1016/j.renene.2019.07.120>
6. Ajbar, A., Lamrani, B., Ali, E. (2023). Dynamic investigation of a coupled parabolic trough collector-phase change material tank for solar cooling process in arid climates. *Energies*, 16(10), 4235. <https://doi.org/10.3390/en16104235>
7. Vijayan, G., Rajasekaran, K. (2020). Performance evaluation of nanofluid on parabolic trough solar collector. *Thermal Science*, 24(2), 853–864. <https://doi.org/10.2298/TSCI200209174V>
8. Singh, S. K., Bhattacharyya, S., Paul, A. R., Sharifpur, M., Meyer, J. P. (2020). Augmentation of heat transfer in a microtube and a wavy microchannel using hybrid nanofluid: A numerical investigation. *Mathematical Methods in the Applied Sciences*. <https://doi.org/10.1002/mma.6849>
9. Wen, D., Ding, Y. (2004). Experimental investigation into convective heat transfer of nanofluids at the entrance region under laminar flow conditions. *International Journal of Heat and Mass Transfer*, 47(24), 5181–5188. <https://doi.org/10.1016/j.ijheatmasstransfer.2004.07.017>
10. Ding, Y., Alias, H., Wen, D., Williams, R. A. (2006). Heat transfer of aqueous suspensions of carbon nanotubes (CNT nanofluids). *International Journal of Heat and Mass Transfer*, 49(1–2), 240–250. <https://doi.org/10.1016/j.ijheatmasstransfer.2005.07.009>
11. Angayarkanni, S. A., Philip, J. (2015). Review on thermal properties of nanofluids: Recent developments. *Advances in Colloid and Interface Science*, 225, 146–176. <https://doi.org/10.1016/j.cis.2015.10.005>
12. Lenin, R., Joy, P. A. (2017). Role of base fluid on the thermal conductivity of oleic acid coated magnetite nanofluids. *Colloids and Surfaces A: Physicochemical and Engineering Aspects*, 529, 922–929. <https://doi.org/10.1016/j.colsurfa.2017.06.065>
13. Jafari, A., Tynjälä, T., Mousavi, S. M., Sarkomaa, P. (2008). Simulation of heat transfer in a ferrofluid using computational fluid dynamics technique. *International Journal of Heat and Fluid Flow*, 29(4), 1197–1202. <https://doi.org/10.1016/j.ijheatfluidflow.2008.01.004>
14. Li, Q., Xuan, Y. (2009). Experimental investigation on heat transfer characteristics of magnetic fluid flow around a fine wire under the influence of an external magnetic field. *Experimental Thermal and Fluid Science*, 33(4), 591–596. <https://doi.org/10.1016/j.expthermflusci.2008.12.013>
15. Lajvardi, M., Moghimi-Rad, J., Hadi, I., Gavili, A., Isfahani, T. D. et al. (2010). Experimental investigation for enhanced ferrofluid heat transfer under magnetic field effect. *Journal of Magnetism and Magnetic Materials*, 322(21), 3508–3513. <https://doi.org/10.1016/j.jmmm.2010.07.002>
16. Sheikholeslami, M., Zeeshan, A., Majeed, A. (2018). Control volume based finite element simulation of magnetic nanofluid flow and heat transport in non-Darcy medium. *Journal of Molecular Liquids*, 268, 354–364. <https://doi.org/10.1016/j.molliq.2018.07.085>
17. Ebrazeh, S., Sheikholeslami, M. (2020). Applications of nanomaterial for parabolic trough collector. *Powder Technology*, 375, 472–492. <https://doi.org/10.1016/j.powtec.2020.07.019>
18. Cao, Y., Bezaatpour, M., Ghaebi, H. (2021). Heat transfer and thermodynamic analysis of individual and simultaneous effects of revolution, microporous media, magnetic inductor, and nanoparticles in concentrating solar collectors. *International Communications in Heat and Mass Transfer*, 129, 105687. <https://doi.org/10.1016/j.icheatmasstransfer.2021.105687>
19. Khosravi, A., Malekan, M., Assad, M. E. (2019). Numerical analysis of magnetic field effects on the heat transfer enhancement in ferrofluids for a parabolic trough solar collector. *Renewable Energy*, 134, 54–63. <https://doi.org/10.1016/j.renene.2018.12.067>
20. Bellos, E., Tzivanidis, C., Antonopoulos, K. A., Gkinis, G. (2016). Thermal enhancement of solar parabolic trough collectors by using nanofluids and converging-diverging absorber tube. *Renewable Energy*, 94, 213–222. <https://doi.org/10.1016/j.renene.2016.03.010>

21. Amani, M., Amani, P., Kasaeian, A., Mahian, O., Wongwises, S. (2017a). Thermal conductivity measurement of spinel-type ferrite  $\text{MnFe}_2\text{O}_4$  nanofluids in the presence of a uniform magnetic field. *Journal of Molecular Liquids*, 230, 121–128. <https://doi.org/10.1016/j.molliq.2017.01.048>
22. Amani, M., Ameri, M., Kasaeian, A. (2017b). The experimental study of convection heat transfer characteristics and pressure drop of magnetite nanofluid in a porous metal foam tube. *Transport in Porous Media*, 116(2), 959–974. <https://doi.org/10.1007/s11242-016-0787-0>
23. Sami, S., Quito, F. (2019). Experimental and numerical study of magnetic field impact on the thermal solar collectors. *International Journal of Sustainable Energy and Environmental Research*, 8(1), 10–28. <https://doi.org/10.18488/journal.13.2019.81.10.28>
24. Xu, G., Zhao, S., Zhang, X., Zhao, X. (2016). Experimental thermal evaluation of a novel solar collector using magnetic nano-particles. *Energy Conversion and Management*, 130, 252–259. <https://doi.org/https://doi.org/10.1016/j.enconman.2016.10.036>